

Iron Optimization for Fenton-Driven Oxidation of MTBE-Spent Granular Activated Carbon

SCOTT G. HULING,*
PATRICK K. JONES, AND TONY R. LEE
Office of Research and Development, National Risk
Management Research Laboratory, U.S. Environmental
Protection Agency, P.O. Box 1198, Ada, Oklahoma 74820

Fenton-driven chemical oxidation of methyl *tert*-butyl ether (MTBE)-spent granular activated carbon (GAC) was accomplished through the addition of iron (Fe) and hydrogen peroxide (H₂O₂) (15.9 g/L; pH 3). The Fe concentration in GAC was incrementally varied (1020–25 660 mg/kg) by the addition of increasing concentrations of Fe solution (FeSO₄·7H₂O). MTBE degradation in Fe-amended GAC increased by an order of magnitude over Fe-unamended GAC and H₂O₂ reaction was predominantly (99%) attributed to GAC-bound Fe within the porous structure of the GAC. Imaging and microanalysis of GAC particles indicated limited penetration of Fe into GAC. The optimal Fe concentration was 6710 mg/kg (1020 mg/kg background; 5690 mg/kg amended Fe) and resulted in the greatest MTBE removal and maximum Fe loading oxidation efficiency (MTBE oxidized (μg)/Fe loaded to GAC(mg/Kg)). At lower Fe concentrations, the H₂O₂ reaction was Fe limited. At higher Fe concentrations, the H₂O₂ reaction was not entirely Fe limited, and reductions in GAC surface area, GAC pore volume, MTBE adsorption, and Fe loading oxidation efficiency were measured. Results are consistent with nonuniform distribution of Fe, pore blockage in H₂O₂ transport, unavailable Fe, and limitations in H₂O₂ diffusive transport, and emphasize the importance of optimal Fe loading.

Introduction

Removal of methyl *tert*-butyl ether (MTBE) from water and subsequent destruction can involve the combined, synergistic use of two reliable and well-established treatment technologies—adsorption onto granular activated carbon (GAC) and Fenton-driven oxidation. MTBE is transformed by hydroxyl radicals (·OH) and other possible reactive species generated during the reaction between H₂O₂ and iron (Fe) immobilized in the GAC. The objectives of the treatment process are to transform adsorbed contaminants into less toxic byproducts, re-establish the sorptive capacity of the carbon for the target chemical(s), increase the useful life of the GAC, and reduce costs for GAC regeneration and water or air treatment.

Fenton's mechanism has been used to regenerate activated carbon loaded with various environmental contaminants: municipal wastewater (1); dimethyl phthalate (2); trichloroethylene (TCE) (3); 2-chlorophenol (4); chlorinated organics (chlorobenzene, tetrachloroethylene, chloroform, 1,2-dichloropropane) (5), *N*-nitrosodimethyl amine (6); and methyl *tert*-butyl ether (MTBE) (7). The most significant

carbon regeneration was measured when the activated carbon was amended with Fe prior to or during Fenton-oxidation regeneration (4–7) which underscores the contribution of Fe to achieve the treatment objectives.

Commercially available GAC contains varying quantities of Fe, depending on the raw materials and on the process used to activate the carbon. Bituminous- and lignite-based GAC contain more Fe than wood- or coconut-based GAC. Additionally, strong chemical oxidants such as phosphoric acid, used during the activation of some carbons can leach metals from the carbon material, thus lowering the Fe content.

It is anticipated that amendment of Fe to GAC will be required in all cases to successfully facilitate the Fenton reaction and to achieve carbon regeneration treatment objectives. Neither the relative contributions of soluble and GAC-bound Fe nor the optimal Fe concentration on the GAC have been previously established. Insufficient Fe loading may prevent adequate Fenton-driven oxidation of the contaminant and prevent successful GAC regeneration treatment. Excessive Fe loading and pore blockage may interfere with contaminant access and H₂O₂ transport to internal pores and sorption sites.

The objective of this study was to optimize the Fe loading on GAC. Despite the high solubility and low sorptive characteristics of MTBE, carbon adsorption is often selected to remove MTBE from water and can be more cost-effective than air stripping (8). The low affinity between MTBE and activated carbon, and the corresponding high carbon usage rates suggest MTBE is a good candidate for the adsorption/oxidation technology investigated here. The rate constant for the reaction between ·OH and MTBE is high (1.6 × 10⁹ L/mol-s) (9), indicating that MTBE is vulnerable to radical attack and transformation in a Fenton system.

Materials and Methods

The GAC used in this study (URV) was supplied by Calgon Carbon Corp. (Pittsburgh, PA). URV is a bituminous-coal-based, 8 × 30 mesh carbon derived from the same starting raw material as commercially available GAC, but was steam activated in a manner designed to minimize H₂O₂ reactivity (10). The as-received GAC was liberally rinsed with deionized (DI) water, dried at 105 °C, and stored in a desiccator at room temperature until used.

Fe Amendment, MTBE Adsorption, and Oxidative Treatment The order of experimental procedures was Fe amendment, MTBE adsorption, and oxidative treatment with H₂O₂. Ferrous sulfate (FeSO₄·7H₂O) was dissolved (20.6 g/L (*n* = 4) as Fe) into DI water. Fe amendment to GAC was carried out by suspending 5 g GAC in 15 mL of Fe solution (0–16.5 g/L Fe). Acidic conditions (pH 2.5) were maintained with dilute H₂SO₄ to maintain soluble Fe in the GAC suspension. A 4-day contact period provided sufficient time for Fe diffusion into the porous structure of the GAC. Subsequently, the pH was raised (pH 3.0) using dilute NaOH. The solution was analyzed for Fe (*n* = 2) and decanted. The term *aqueous Fe* ([Fe]_{AQ}) refers to the soluble + colloidal particulate in solution and *GAC-bound Fe* refers to the Fe anchored to, or immobilized within the GAC.

Adsorption was carried out in batch mode by amending MTBE solutions (0.12 L, 1.88 mg/L) to 5 g of GAC (>7 day contact time) contained in 10 parallel reactors. MTBE adsorption and MTBE oxidation were carried out in Erlenmeyer flasks wrapped in aluminum foil and covered with Parafilm. Pre- and post-adsorption aqueous samples were analyzed to quantify the mass of MTBE sorbed. Oxidation

* Corresponding author phone: (580) 436-8610; fax: (580) 436-8614; e-mail: huling.scott@epa.gov.

TABLE 1. Pre-Oxidation Results of Fe Amendment to the GAC^a

reactor	initial ^b [Fe] _{AQ} (g/L)	final [Fe] _{GAC} ^c (mg/kg)	final ^d [Fe] _{AQ} (mg/L)	fraction ^e retained (%)
A	0 (background)	1020 (980–1070)	2	
B	1.1	4270 (3930–4620)	29	97
C	2.2	6710 (6650–6770)	44	98
D	3.3	9640 (9360–9910)	56	98
E	4.4	12 630 (12 320–12 940)	97	98
F	5.5	15 760 (15 390–16 130)	270	95
G	6.6	16 900 (16 440–17 360)	730	89
H	8.2	18 520 (18 470–18 570)	1590	81
I	12.3	23 500 (22 020–24 980)	3900	68
J	16.5	25 660 (25 530–25 790)	5700	65

^a Background [Fe] = 1020 mg/kg, [Mn]_{GAC} = 9 mg/kg (*n* = 3); 95% confidence interval (C.I.) (mg/kg) 9–10 mg/kg. ^b 15 mL of aqueous Fe solution (pH 2.5) applied to 5 g of GAC. ^c 95% C.I. in parenthesis (*n* = 3). ^d Post Fe-amendment solution (pH 3) (before decanting step). ^e Mass fraction of Fe retained after treatment ((Initial [Fe]_{AQ} – Final [Fe]_{AQ})/Initial[Fe]_{AQ}) × 100.

was carried out by amending H₂O₂ to the GAC in 3 sequential applications (1.91 mL of 30% H₂O₂ per application; [H₂O₂] = 15.9 g/L). This approach reduced spikes in H₂O₂ concentration and •OH scavenging by H₂O₂. Reactors were placed on an orbital shaking table (100 rpm) only during the reaction of H₂O₂. During oxidation, the pH was held constant (pH 3.0). Control reactors (*n* = 4) were used to differentiate between H₂O₂ reaction with aqueous Fe versus GAC-bound Fe. GAC-free control reactors contained 45 mg/L Fe (40 mL volume) (pH 3) and were amended with 1.91 mL of 30% H₂O₂. Volatile emissions of MTBE were vented via flow-through GAC traps mounted on the reactors. The GAC was extracted and analyzed, and MTBE losses from the test reactors were negligible (data not shown).

Time-dependent H₂O₂ concentrations were measured (*n* = 3) in 4 of the 10 test reactors to quantify the H₂O₂ degradation rate. Upon complete reaction of H₂O₂, post-oxidation samples of the aqueous solution in the reactors were analyzed for total Fe (Fe_T) (*n* = 2), pH, MTBE (*n* = 2), and degradation byproducts (*n* = 2). Post-oxidation GAC samples were extracted and analyzed for MTBE, TBA, and acetone (*n* = 2). Pre- and post-oxidation GAC samples were dried (105 °C; 24 h) and measured in duplicate for surface area, pore volume distribution (microporosity, meso + macroporosity, total porosity), and metals.

Analytical. Analytical methods and materials used in the measurement of GAC metals, GAC surface area and pore volume, aqueous phase and GAC MTBE, imaging and microanalysis of GAC particles (scanning electron microscopy (SEM)/energy dispersive X-ray spectrometry (EDS)), H₂O₂, iron, and pH are available in the Supporting Information (SI).

Results

Iron Amendment to GAC. The Fe concentration on the GAC ([Fe]_{GAC}) ranged from background to over 25 times the background concentration (Table 1). Iron retained was from precipitation, ion exchange, and complexation reactions and was inversely proportional to the initial Fe concentration in solution applied to the GAC indicating a saturation effect. The background manganese (Mn) concentration was low (9 mg/kg) relative to Fe (1020 mg/kg) (Table 1). In Fenton systems, Mn catalyzes H₂O₂ reactions, but •OH are not produced, thus a potential source of treatment inefficiency. Due to the low Mn content relative to Fe, Mn was not a significant source of process inefficiency. Further, significant increases in the H₂O₂ reaction rate corresponding with Fe amendments to GAC (discussed below) indicates H₂O₂ reaction is predominantly attributed to Fe and not Mn.

The post-oxidation N₂ BET surface area and total pore volume of the GAC were inversely related to the mass of Fe

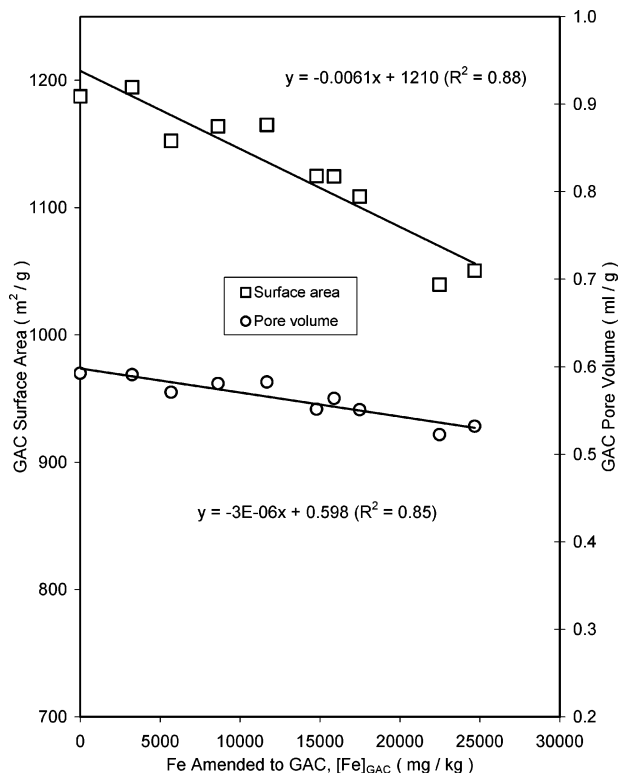


FIGURE 1. Inverse correlation between the quantity of Fe added to the GAC and the GAC surface area and pore volume. The carbon (URV, Calgon Carbon) has a surface area of 1190 m²/g (95% C.I. 1110–1270 m²/g) and a total pore volume of 0.59 mL/g (95% C.I. 0.52–0.66 mL/g).

amended to the GAC (Figure 1). Approximately 31 m²/g and 0.015 mL/g loss in N₂ BET surface area and pore volume, respectively, were measured per 5000 mg/kg of Fe amended to the GAC. This represents a 2–3% decline of the original surface area (1290 m²/g) and pore volume (0.64 mL/g) of the URV GAC. Repeated oxidative treatments of GAC with H₂O₂ can result in reductions in N₂ BET surface area, pore volume, and sorptive capacity (11). These effects are significantly reduced when loaded with a target compound such as MTBE (7).

MTBE Oxidation. The positive correlation established between the pre-oxidation aqueous MTBE concentration and the Fe concentration on the GAC suggests that Fe accumulation in the GAC interfered with MTBE adsorption (Figure 2). Pore throat blockage by Fe may have limited transport to the internal porosity and surface area of the GAC. Despite the increase in [MTBE]_{AQUEOUS} with increasing [Fe]_{GAC}, only minor reductions in the MTBE loading rate on

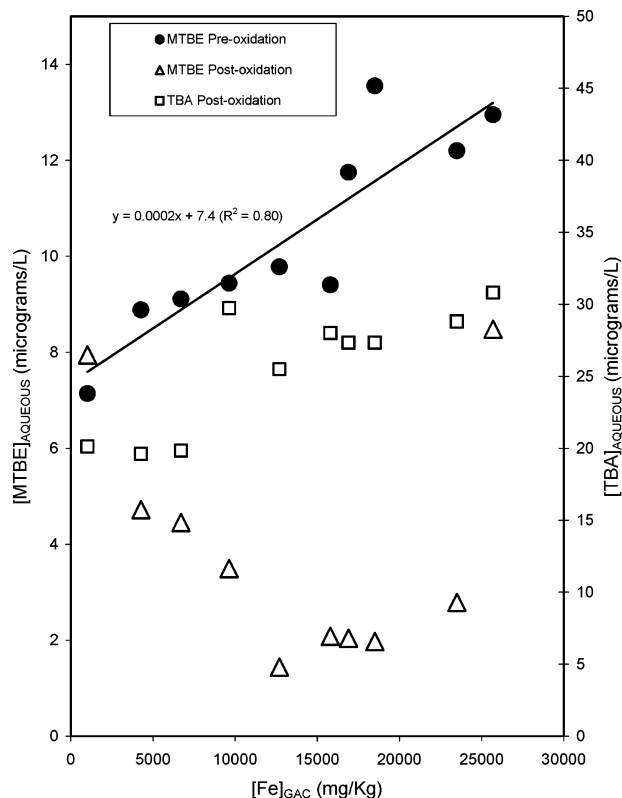


FIGURE 2. Pre-oxidation MTBE and post-oxidation MTBE and TBA concentrations in GAC relative to the Fe concentration on the GAC.

TABLE 2. Post-Sorption and Post-Oxidation MTBE Concentrations in the GAC ([MTBE]_{GAC}) (Initial Conditions: 0.12 L, 1.88 mg/L MTBE, 5 g GAC)

reactor	post-sorption (pre-oxidation) initial [MTBE] _{GAC} (mg/kg) ^a	post-oxidation final [MTBE] _{GAC} (mg/kg)	removal of MTBE from GAC (%) ^b
A	41.3	40.6	2
B	41.2	38.1	8
C	41.1	29.3	29
D	40.9	31.0	24
E	40.9	33.2	19
F	40.9	31.7	23
G	41.0	29.6	28
H	40.7	33.9	17
I	40.9	31.6	23
J	41.0	31.5	23

^a Sampling losses were accounted for in the initial [MTBE]_{GAC}.

^b Average percent removal = $100 \times (\text{Initial [MTBE]}_{\text{GAC}} - \text{Final [MTBE]}_{\text{GAC}}) / (\text{Initial [MTBE]}_{\text{GAC}})$ ($n = 2$).

Fe-amended GAC ([MTBE]_{GAC}) were measured (<1% reduction in loading) (Table 2).

Post-oxidation aqueous analysis indicated a declining trend in the MTBE concentration and an increase in TBA, a reaction byproduct from MTBE oxidation (Figure 2). No acetone was measured in solution. High concentrations of acetone and TBA measured in the methanol solvent blank prevented an accurate measure of acetone and TBA extracted from the GAC. Negligible accumulation of these reaction products was measured on identical GAC under similar conditions involving Fenton oxidation of activated carbon (7).

Oxidation of MTBE increased by an order of magnitude over background from the amendment of Fe (Table 2). The optimal Fe loading was approximately 6710 mg/kg Fe (reactor C, 5690 mg/kg amended Fe) where the highest MTBE removal

was measured, relative to background (reactor A, Fe-amended GAC), and where the highest Fe loading oxidation efficiency (MTBE oxidized (μg)/Fe loaded to GAC (mg/kg)) was measured (Figure 3). The treatment objective was to add sufficient H₂O₂ to ensure a moderate level of MTBE oxidation and to provide results which could distinguish between GAC regeneration attributed to different levels of Fe. More applications of H₂O₂ could have accomplished a greater level of MTBE oxidation and GAC regeneration, but was not a treatment objective.

H₂O₂ Reaction. H₂O₂ reaction was pseudo-first order, similar to other heterogeneous systems (4, 12–13), and a positive relationship was established between the pseudo-first-order H₂O₂ reaction rate constant (k_T) and [Fe]_{GAC} (Figure 4, eqs 1 and 2). A nonlinear relationship between Fe content and H₂O₂ reaction (i.e., saturation effect) was observed between 6710 mg/kg total Fe (5690 mg/kg amended Fe) and 15 760 mg/kg (14 740 mg/kg amended Fe), indicating that H₂O₂ reaction was not entirely Fe limited and that other mechanisms limited H₂O₂ reaction.

H₂O₂ reaction occurs with both Fe in the aqueous phase (soluble + suspended particulate) and GAC-bound Fe (eq 1). Substituting k_T into eq 1 and integrating yields a form of the equation that can be used to evaluate k_T (eqs 2–4). The H₂O₂ reaction rate constants (Figure 4) calculated from semilog plots (not shown) of H₂O₂ concentration versus time represent the combined pseudo first-order reaction rate constant (k_T).

$$-dC/dt = k_{AQ}C + k_{GAC}C \quad (1)$$

$$k_T = k_{AQ} + k_{GAC} \quad (2)$$

$$-dC/dt = k_T C \quad (3)$$

$$\ln C(t) = \ln C_0 - k_T t \quad (4)$$

where k_{AQ} = pseudo first-order H₂O₂ reaction rate constant involving aqueous Fe (hr⁻¹), k_{GAC} = pseudo first-order H₂O₂ reaction rate constant involving GAC-bound Fe (hr⁻¹), k_T = pseudo first-order (combined) H₂O₂ reaction rate constant (hr⁻¹), C_0 = initial H₂O₂ concentration in solution (mg/L), $C(t)$ = time-dependent H₂O₂ concentration in solution (mg/L), and t = time (hr) ($t = t_0$; $C = C_0$).

The post-oxidation aqueous Fe concentrations in reactors A (2.9 mg/L), C (10.3 mg/L), F (27.1 mg/L), and J (44.8 mg/L) were low and accounted for 2–3% of the total Fe in each reactor. Reactor J exhibited the highest aqueous Fe concentration (44.8 mg/L) and thus represented the greatest potential for aqueous Fe reaction with H₂O₂. Replicate control reactors without GAC were prepared to simulate and measure H₂O₂ degradation in reactor J (45 mg/L Fe; pH 3; 1.91 mL of 30% H₂O₂; 40 mL solution) and to assess the relative contributions of aqueous and GAC-bound Fe in the H₂O₂ reaction. The pseudo first-order H₂O₂ degradation rate constant in these control reactors (i.e., k_{AQ}) was 0.13 h⁻¹ ($n = 4$). Using eq 2, k_{AQ} , and k_T for reactor J (11.4 h⁻¹), k_{GAC} was determined to be 11.27 h⁻¹. Results indicate aqueous Fe contributed only 1% to the combined H₂O₂ degradation rate constant. Since aqueous Fe in other test reactors accounted for approximately the same fraction of total Fe (i.e., 2–3%), the contribution of aqueous Fe to H₂O₂ reaction was concluded to be negligible in all reactors. Fenton-dependent H₂O₂ consumption was dominated by reaction with GAC-bound Fe in all cases and the majority of H₂O₂ consumption occurred within the porous structure of the GAC. This is a favorable outcome since H₂O₂ and •OH reaction occurred at or near the carbon surface. Under this condition, sorbed MTBE and high soluble concentrations of MTBE near the GAC surface have a greater probability of reacting with •OH.

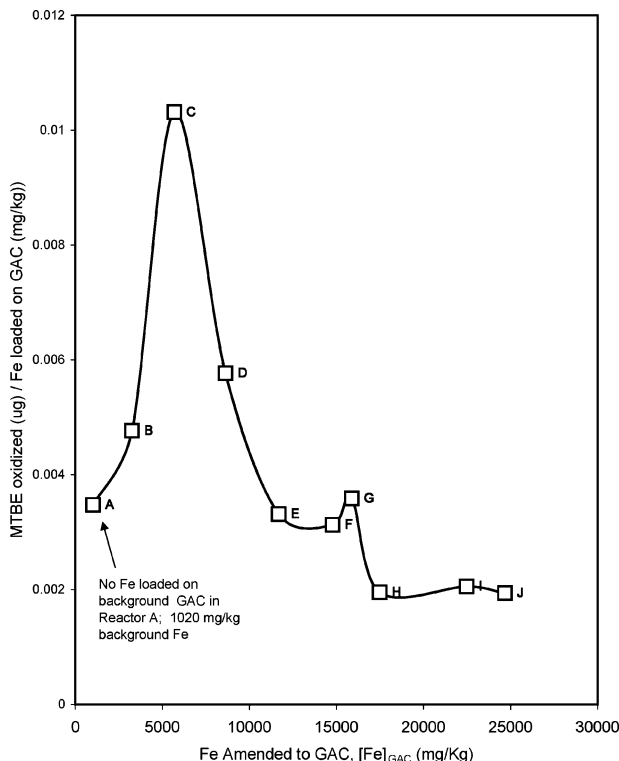


FIGURE 3. MTBE degraded in the GAC is functionally dependent on the Fe concentration in GAC (see also, Table 2). The Fe amended to the GAC was calculated by the difference between the background (1020 mg/kg) and final Fe concentrations in the GAC (see Table 1).

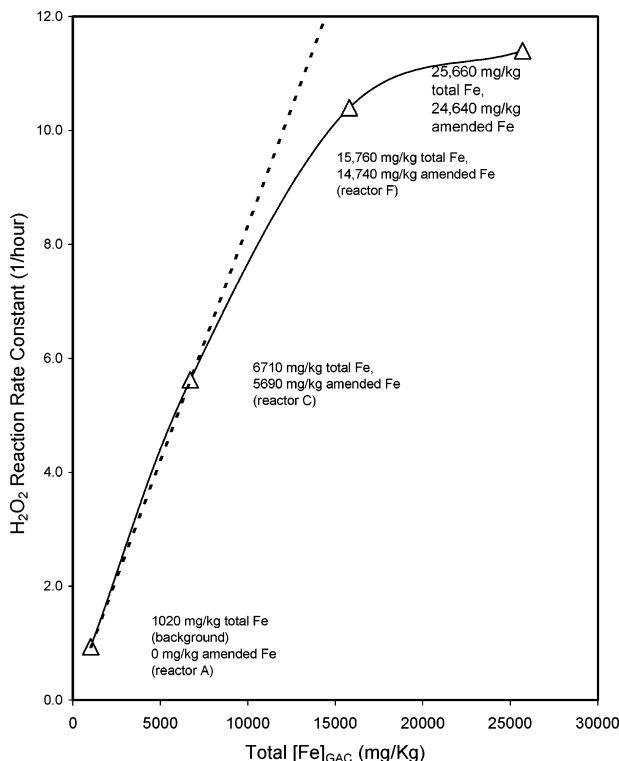


FIGURE 4. Nonlinear relationship between total Fe (background + amended) and the pseudo first-order H_2O_2 degradation rate constant (k_T) (average k_T ; $n = 3$; $r^2 > 0.9$).

Scanning Electron Microscopy (SEM)/Energy Dispersive X-ray Spectrometry (SEM/EDS). Analysis of Fe-amended GAC particles by SEM/EDS provided quantitative information on Fe distribution in the GAC. Post-oxidation analysis of GAC particles by SEM/EDS indicated an increase in the

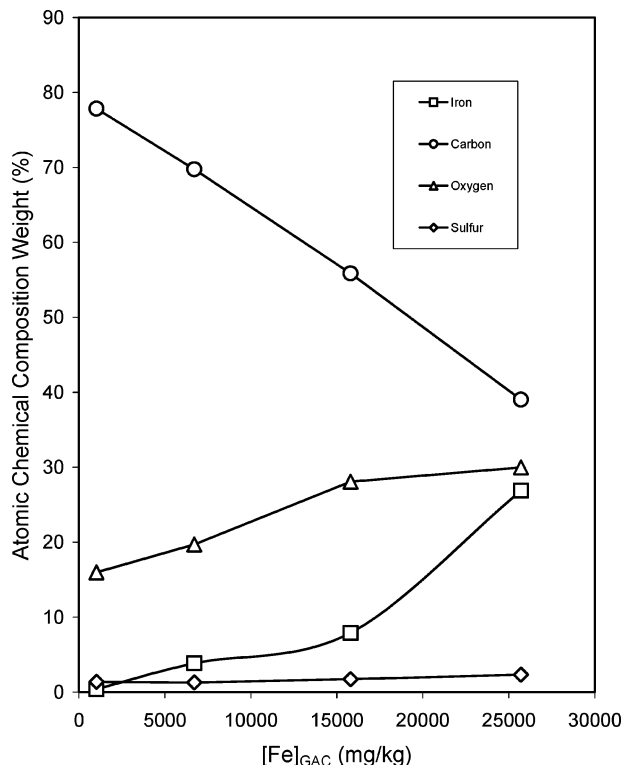


FIGURE 5. Atomic chemical composition weight in Fe-amended GAC (see Table 1, reactors A, C, F, J) measured by SEM/EDS (20 keV acceleration voltage).

surface atomic chemical composition weight of Fe, O, and S and a simultaneous decline in C (Figure 5).

The electron range in EDS measurements is the distance traveled by the incident (beam) electrons within the specimen being analyzed (14). The Kanaya–Okayama electron range (R_{KO}) (eq 5) is equivalent to the radius of a circle centered on the surface at the beam impact point of the specimen whose circumference encompasses the limiting envelope of the interaction volume (14). R_{KO} provides a numerical estimate of the depth dimension in the interaction volume.

$$R_{KO} = 0.0276 A E_0^{1.67} / Z^{0.89} \rho \quad (5)$$

where A = atomic weight (carbon = 12.01 g/mol), E_0 = incident beam energy (keV), Z = atomic number (carbon = 6), and ρ = density (graphite carbon = 2.25 g/cm³).

R_{KO} was 0.4, 1.4, 4.5, and 8.8 μm at 5, 10, 20, and 30 keV, respectively, for graphitic carbon. The interrogation depth of the beam electron was approximately 18 μm (i.e., $2 \times 8.8 \mu\text{m}$). The acceleration voltage was varied over a similar range (5–30 keV) for Fe-amended GAC (reactor F; [Fe] = 16 500 mg/kg). The inverse relationship between the Fe and C chemical composition suggests that the Fe amended to the GAC was immobilized within a short transport distance (18 μm) within the GAC particle (Figure 6). Since the chemical composition weight is a depth averaged measurement, the Fe levels are estimated to be at or near the background level (0.41%) at the 18 μm penetration depth in the GAC. Neither C nor Fe varied in surface atomic composition weight in Fe-unamended GAC over the range of acceleration voltage tested (5–30 keV).

Discussion

Fe Loading. Fe amendment to GAC is required to enhance MTBE oxidation. Low Fe loading could result in lower MTBE oxidation efficiency, and higher post-regeneration concen-

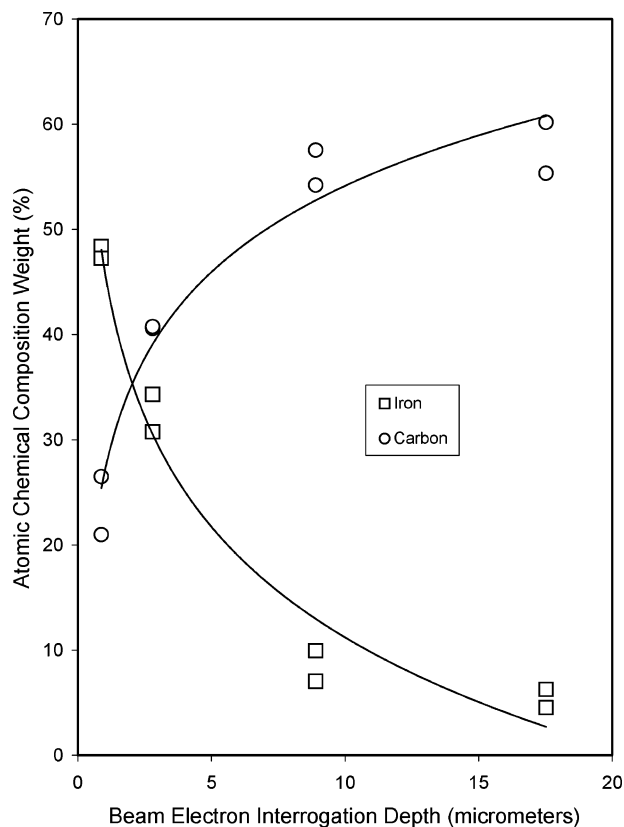


FIGURE 6. Atomic chemical composition weight in Fe-amended GAC measured by SEM/EDS derived from varying the accelerating voltage (5, 10, 20, 30 keV), (Reactor F: [Fe] = 15 760 mg/kg).

trations of MTBE. Here, Fe loading at any level resulted in loss of surface area and pore volume and therefore, must be optimally balanced to minimize undesirable effects. In a previous study involving similar GAC and Fe amendment procedures, selective chemical extraction of the Fe-amended GAC indicated that the freshly added Fe was predominantly amorphous Fe (11). Colloidal amorphous Fe has limiting diameters between 2 and 8 nm (15) suggesting that even the smallest Fe particles are large enough to block micropores in GAC with diameters typically <2 nm. Reduction in the surface area and iodine number (i.e., a general indicator of microporosity) in lignite-based GAC was attributed to Fe amendment and the accumulation of Fe oxides in pore throats of micropores (16). Overall, the optimal total Fe concentration was approximately 6710 mg/kg (1020 mg/kg background Fe, and 5690 mg/kg amended Fe) (Figure 3) and MTBE removal at Fe concentrations above 5690 mg/kg was greater than MTBE removal in the unamended control (background), but was not optimal.

MTBE Oxidation. Competition kinetics between $\cdot\text{OH}$ and two probable reactants in the aqueous phase, MTBE and H_2O_2 , was analyzed to assess the relative reaction and oxidation efficiency. The MTBE reaction rate constant is 60 times greater than H_2O_2 (reactions 1 and 2); however, very high concentrations of H_2O_2 (15.9 g/L; 0.44 M) were present in the GAC slurry relative to MTBE (7–13 $\mu\text{g}/\text{L}$; 7.9×10^{-5} to 1.5×10^{-4} mmol) (Table 2). Here, it was assumed that $[\cdot\text{OH}]$ was the same in the two reaction rate equations (eqs 6 and 7) since the reactants were present in a common reactor. The relative rate of reaction (R_R) (eq 8) indicates that $\cdot\text{OH}$ reacts more rapidly with H_2O_2 (i.e., $R_R = 50\,000$) than with MTBE. Even at lower H_2O_2 concentration (150 mg/L), R_R is 500, indicating that H_2O_2

scavenging of $\cdot\text{OH}$ over a wide concentration range is dominant relative to the reaction between $\cdot\text{OH}$ and MTBE.

$\cdot\text{OH} + \text{MTBE} \rightarrow \text{products}$

$$k_1 = 1.6 \times 10^9 \text{ M}^{-1} \text{ s}^{-1} \quad (9) \text{ (rxn 1)}$$

$\cdot\text{OH} + \text{H}_2\text{O}_2 \rightarrow \text{products}$

$$k_2 = 2.7 \times 10^7 \text{ M}^{-1} \text{ s}^{-1} \quad (9) \text{ (rxn 2)}$$

$$-\text{d}[\text{MTBE}]/\text{d}t = k_1 [\text{MTBE}] [\cdot\text{OH}] \quad (6)$$

$$-\text{d}[\text{H}_2\text{O}_2]/\text{d}t = k_2 [\text{H}_2\text{O}_2] [\cdot\text{OH}] \quad (7)$$

Relative rate of reaction (R_R) =

$$\frac{\text{d}[\text{H}_2\text{O}_2]/\text{d}t}{\text{d}[\text{MTBE}]/\text{d}t} = \frac{k_2 [\text{H}_2\text{O}_2]}{[\cdot\text{OH}]/k_1 [\text{MTBE}] [\cdot\text{OH}]} \approx 50,000 \quad (8)$$

This simplified kinetic analysis does not account for high MTBE concentrations and reaction in the aqueous phase that may occur near the carbon surface (i.e., thin film), or $\cdot\text{OH}$ oxidation of sorbed MTBE.

The overall oxidation efficiency (η) (eq 9) is the product of efficiencies associated with (1) the ratio of Fenton-dependent $\cdot\text{OH}$ formation to the total H_2O_2 consumed in Fenton and non-Fenton reactions (E_1), and (2) the ratio of MTBE transformed by $\cdot\text{OH}$ to the total $\cdot\text{OH}$ consumed in all reactions (E_2) (13).

$$\eta = E_1 \times E_2 \times 100 \quad (9)$$

A decline in E_1 and E_2 results from nonproductive H_2O_2 reactions that do not produce $\cdot\text{OH}$, and $\cdot\text{OH}$ scavenging reactions, respectively. Raising the Fe content of the GAC increased MTBE oxidation (Table 2), the H_2O_2 reaction rate constant and correspondingly, reduced nonproductive reactions and E_1 . E_2 is the probable primary source of oxidation inefficiency because $\cdot\text{OH}$ scavenging resulted from using high concentrations of H_2O_2 and from the oxidation of reaction byproducts including TBA and acetone.

The optimal H_2O_2 concentration in heterogeneous treatment systems involving Fe(III) is dependent on various factors including the contaminant sorption characteristics (i.e., octanol water partition coefficient), scavenging by soil and dissolved constituents (17), soil organic carbon content, pH, the rate of reaction between contaminant and $\cdot\text{OH}$ (18), mineral type, and surface area (19). Additionally, high H_2O_2 concentrations promote propagation reactions that form transient reactive oxygen species other than $\cdot\text{OH}$ that aid in the destruction of organic contaminants (18). Consequently, these factors, and probably others, play a role in the optimal H_2O_2 concentration in GAC regeneration for each set of chemical and physical conditions encountered. The initial H_2O_2 concentration in our study was held constant (15.9 g/L) under all testing conditions and H_2O_2 concentration was not independently investigated.

H_2O_2 Reaction. The kinetic analysis of H_2O_2 reaction developed in this study successfully differentiated between the aqueous- and solid-phase reactions. Through this analysis, it is clear that H_2O_2 reaction occurs predominantly within the GAC and not in solution. The nonlinear relationship between the Fe content in GAC and the H_2O_2 reaction rate constant (Figure 4) indicated that H_2O_2 reaction was not entirely Fe limited at higher Fe concentration and other mechanisms played a role in limiting H_2O_2 reaction. Fe blockage of H_2O_2 transport, unavailable Fe, and the effect of fast H_2O_2 reaction rates on H_2O_2 diffusive transport are proposed mechanisms. The post-oxidation total pore volume (0.593 mL/g) (Figure 1) of the Fe-unamended GAC (i.e.,

reactor A) is comprised mainly of micropore volume (0.405 mL/g) and to a lesser extent, mesopore + macropore volume (0.188 mL/g). Fe precipitation and deposition (i.e., amorphous ferrihydrite) resulted in the accumulation of colloidal Fe within the porous structure of the GAC and, consequently, a reduction in pore volume and surface area. The high H₂O₂ reaction rate in conjunction with pore blockage by Fe may have limited the diffusive transport of H₂O₂ and penetration into the GAC. Collectively, these mechanisms would limit contact between H₂O₂, GAC surface area, Fe, and the adsorbate. Reductions in the surface area and pore volume of the GAC (Figure 1), MTBE adsorption (Figure 2), and in Fe loading oxidation efficiency from high Fe loading (Figure 3), are consistent with a conceptual model of nonuniform distribution of Fe, pore blockage, and greater tortuosity in H₂O₂ diffusive transport through the narrow, Fe-rich interval on the periphery of the GAC.

SEM/EDS. Acidic treatment of GAC during Fe-amendment and oxidative treatments during Fenton regeneration can promote substantial alterations to activated carbon surface functionality (20). For example, treatment of coal-based GAC caused a significant increase in acidic surface oxides using nitric acid (>600%) (20) and H₂O₂ (150%) (11). Acidic functional groups formed from acidic and/or oxidative treatment at the edges of the graphene planes exhibit high oxygen content and impart cation exchange capacity to the GAC aiding in the immobilization of Fe. The increase in oxygen composition measured in the GAC (Figure 5) is also attributed to the oxygen content in Fe oxides and sulfate immobilized within the GAC. The majority of the sulfate anion from FeSO₄·7H₂O amended to the GAC was eliminated during the pretreatment rinsing step and low quantities of sulfate were retained (Figure 5).

The range in diameter of GAC particles (8 × 30) used in this study is approximately 600–2400 μm. Assuming a spherical shape of GAC, the 18–20 μm penetration depth of Fe into the GAC particles accounts for 4–19% of the volume. Loss of surface area, pore volume (Figure 1), and MTBE sorption capacity (Figure 2) measured in the GAC are likely attributed to the abundance of Fe immobilized within the narrow interval. Given the limited penetration of Fe into the GAC, data suggest the majority of MTBE did not reside in the Fe-rich zone of the GAC, and the majority of H₂O₂ and ·OH reacted within the narrow, Fe-rich interval on the periphery of the GAC particle. Under this condition, MTBE oxidation requires that MTBE desorb from the GAC interior and diffuse to the exterior of the GAC particle where Fe is abundant and the majority of H₂O₂ reaction occurs. Low concentrations of MTBE in the Fe-rich zone results in a steep, outward concentration gradient resulting in mass transfer and transport of MTBE from the GAC interior to the exterior of the GAC particle. This conceptual model is consistent with De La Casas et al. (21) who reported that the rates of contaminant desorption and oxidation were similar in GAC and that Fenton-driven regeneration of GAC is limited by intra-particle mass transport (diffusion) of the target compound and not by reaction rate.

Other. The optimal [Fe]_{GAC} observed for MTBE oxidation in URV GAC in this study may not be optimal for other contaminant/GAC combinations. For example, other types of activated carbon exhibit variability in porous structure and surface chemistry. Attachment and distribution of Fe in other carbon may vary accordingly. The form of Fe used in Fenton oxidation may also influence the rate of H₂O₂ reaction, ·OH production, and contaminant oxidation (22) but was not investigated in this study.

We acknowledge J. Andrews (East Central University, Ada, OK), S. Beach, M. Blankenship, Dr. G. Jungclaus, W. Mixon, Dr. N. Xu (Shaw Environmental Inc., Ada, OK), and Dr. Bruce Pivetz (Dynamac Corp., Ada, OK) for their assistance. The

U.S. Environmental Protection Agency, through its Office of Research and Development, funded and managed the research described here. It has not been subjected to Agency review and therefore does not necessarily reflect the views of the Agency, and no official endorsement should be inferred.

Supporting Information Available

Additional details of analytical methods used in this research. This material is available free of charge via the Internet at <http://pubs.acs.org>.

Literature Cited

- (1) Johnson, R. L.; Lowes, F. J., Jr.; Smith, R. M.; Powers, T. J. *Evaluation of the Use of Activated Carbons and Chemical Regenerants in Treatment of Waste Water*; Public Health Service Publication No. 999-WP-13; U.S. Department of Health, Education, and Welfare: Washington, DC, 1964; 48 pp.
- (2) Ashcroft, C. T.; Borup, M. B. Chemical regeneration of granular activated carbon with hydrogen peroxide. In *Proceedings of the American Water Works Association Annual Conference*, Vancouver B.C., 1992; pp 191–200.
- (3) Mourand, J. T.; Crittenden, J. C.; Hand, D. W.; Perram, D. L.; Notthakun, S. Regeneration of spent adsorbents using homogeneous advanced oxidation. *Water Environ. Res.* **1995**, *67* (3), 355–363.
- (4) Huling, S. G.; Arnold, R. G.; Sierka, R. A.; Jones, P. K.; Fine, D. Contaminant adsorption and oxidation via Fenton reaction. *J. Environ. Eng.* **2000**, *126* (7), 595–600.
- (5) Toledo, L. C.; Silva, A. C. B.; Augusti, R.; Lago, R. M. Application of Fenton reagent to regenerate activated carbon saturated with organochloro compounds. *Chemosphere* **2003**, *50*, 1049–1054.
- (6) Kommineni, S.; Ela, W. P.; Arnold, R. G.; Huling, S. G.; Hester, B. J.; Betterton, E. A. NDMA treatment by sequential GAC adsorption and Fenton-driven destruction. *J. Environ. Eng. Sci.* **2003**, *20* (4), 361–373.
- (7) Huling, S. G.; Jones, P. K.; Ela, W. P.; Arnold, R. G. Fenton-driven chemical regeneration of MTBE-spent granular activated carbon. *Water Res.* **2005**, *10* (39), 2145–2153.
- (8) Wilhelm, M. J.; Adams, V. D.; Curtis, J. G.; Middlebrooks, E. J. Carbon adsorption and air-stripping removal of MTBE from river water. *J. Environ. Eng.* **2002**, *128* (9), 813–823.
- (9) Buxton, G. V.; Greenstock, C.; Hellman, W. P.; Ross, A. B. Critical review of rate constants for reactions of hydrated electrons, hydrogen atoms, and hydroxyl radicals (·OH/·O⁻) in aqueous solution. *J. Phys. Chem. Ref. Data.* **1988**, *17* (2), 513–886.
- (10) Hayden, R. Calgon Carbon Corporation, Pittsburgh, PA, 2001, Personal Communication.
- (11) Huling, S. G.; Jones, P. K.; Ela, W. P.; Arnold, R. G. Repeated reductive and oxidative treatments on granular activated carbon. *J. Environ. Eng.* **2005**, *131* (2), 287–297.
- (12) Huling, S. G.; Arnold, R. G.; Jones, P. K.; Sierka, R. A. Contaminant adsorption and oxidation via Fenton reaction. *J. Environ. Eng.* **2000**, *126* (4), 348–353.
- (13) Huling, S. G.; Arnold, R. G.; Sierka, R. A.; Miller, M. Measurement of hydroxyl radical activity in a soil slurry using 4POBN. *Environ. Sci. Technol.* **1998**, *32* (21), 3436–3441.
- (14) Kanaya, K.; Okayama, S. Penetration and energy-loss theory of electrons in solid targets. *J. Phys. D.:Appl. Phys.* **1972**, *5*, 43.
- (15) Cornell, R. M.; Giovanoli, R.; Schneider, W. Review of the hydrolysis of Iron(III) and the crystallization of amorphous iron(II) hydroxide hydrate. *J. Chem. Technol. Biotechnol.* **1989**, *46*, 115–134.
- (16) Reed, B. E.; Vaughan, R.; Jiang, L. As(III), As(V), Hg, and Pb removal by Fe-oxide impregnated activated carbon. *J. Environ. Eng.* **2000**, *126* (9), 869–873.
- (17) Quan, H. N.; Teel, A. L.; Watts, R. J. Effects of contaminant hydrophobicity on H₂O₂ dosage requirements in the Fenton-like treatment of soils. *J. Hazard. Mater.* **2003**, *2–3* (102), 277–289.
- (18) Watts, R. J.; Teel, A. L. Chemistry of modified Fenton's reagent (catalyzed H₂O₂ propagations - CHP) for in-situ and soil and groundwater remediation. *J. Environ. Eng.* **2005**, *4* (131), 612–622.
- (19) Kwan, W. P.; Voalfer, B. M. Rates of hydroxyl radical generation and organic compound oxidation in mineral-catalyzed Fenton-like systems. *Environ. Sci. Technol.* **2003**, *6* (37), 1150–1158.

- (20) Karanfil, T.; Kilduff, J. E. Role of granular activated carbon surface chemistry on the adsorption of organic compounds. 1. Priority pollutants. *Environ. Sci. Technol.* **1999**, *33* (18), 3217–3224.
- (21) De Las Casas, C.; Bishop, K.; Bercik, L.; Johnson, M.; Potzler, M.; Ela, W.; Sáez, A. E.; Huling, S.; Arnold, R. In-Place Regeneration of GAC using Fenton's Reagents. In *Innovative Approaches for the Remediation of Subsurface-Contaminated Hazardous Waste Sites: Bridging Flask and Field Scales*; Clark, C., Lindner, A., Eds.; ACS Symposium Series 940; American Chemical Society: Washington, DC, 2006; pp 43–65.
- (22) De Laat, J. D.; Le, G. T.; Legube, B. A comparative study of the effects of chloride, sulfate, and nitrate ions on the rates of decomposition of H_2O_2 and organic compounds by $\text{Fe(II)}/\text{H}_2\text{O}_2$ and $\text{Fe(III)}/\text{H}_2\text{O}_2$. *Chemosphere* **2004**, *5* (55), 715–723.

Received for review November 6, 2006. Revised manuscript received March 15, 2007. Accepted March 16, 2007.

ES062666K